# Carbon-Supported Pt–Co Catalysts Prepared by a Modified Polyol Process as Cathodes for PEM Fuel Cells

**ARTICLE** *in* THE JOURNAL OF PHYSICAL CHEMISTRY C · FEBRUARY 2007

Impact Factor: 4.77 · DOI: 10.1021/jp0670081



**3 AUTHORS**, INCLUDING:

Laudemir C. Varanda
University of São Paulo
**31** PUBLICATIONS **406** CITATIONS

SEE PROFILE

Hebe de las Mercedes Villullas
São Paulo State University
**44** PUBLICATIONS **711** CITATIONS

SEE PROFILE

# Carbon-Supported Pt−Co Catalysts Prepared by a Modified Polyol Process as Cathodes for PEM Fuel Cells

**Elisabete I. Santiago,† Laudemir C. Varanda, and H. Mercedes Villullas***

*Departamento de Físico Química, Instituto de Química, Universidade Estadual Paulista (UNESP), 14801-970 CP 355, Araraquara (SP), Brazil*

*Received: October 25, 2006; In Final Form: January 4, 2007*

In this work, carbon-supported $Pt_{70}Co_{30}$ nanoparticles were prepared by a polyol process using a long-chain diol as reducer (hexadecanediol) and oleic acid and oleylamine as stabilizers. Depending on the synthesis conditions, $Pt_{70}Co_{30}$/C nanocatalysts with very small particle size ($1.9 \pm 0.2$ nm) and narrow distribution homogeneously dispersed on the carbon support and having a high degree of alloying without the need of thermal treatments were obtained. The as-prepared catalyst presents an excellent performance as proton exchange membrane fuel cells (PEMFC) cathode material. In terms of mass activity (MA), the $Pt_{70}Co_{30}$/C electrocatalysts produced single fuel cell polarization response superior to that of commercial catalyst. To analyze alloying effects, the result of thermal treatment at low temperatures (200−400 °C) was also evaluated and an increase of average crystallite size and a lower degree of alloying, probably associated to cobalt oxidation, were evidenced.

## Introduction

The development of new materials with high surface area, good catalytic properties, and stability, as well as the improvement of their preparation methods, is still needed to increase the efficiency of many technologically relevant processes. Among others, the conversion of chemical energy into electricity in proton exchange membrane fuel cells (PEMFC) requires the development of better electrocatalyst to improve the cell performance. One of the key factors affecting the PEMFC performance is the slow kinetics of the oxygen reduction reaction (ORR), responsible for overpotential losses of ∼0.3−0.4 V under typical conditions of operation.[1]

Among all pure metals, Pt exhibits the highest catalytic activity for the ORR. Platinum supported on high surface area carbon is generally used as electrocatalyst for PEMFC cathodes. However, to further reduce the voltage losses associated to the cathode performance, it is necessary to develop ORR electrocatalysts more active than platinum. With this purpose, several Pt-based binary systems, such as Pt−Fe,[2−10] Pt−Mn,[2] Pt−Cu,[5,9] Pt−Ni,[2,4,5,9,11−18] Pt−Co,[2,4,5,8−10,16−27] Pt−Cr,[2,18,28−32] and Pt−V,[33,34] with different Pt:M atomic compositions have been investigated and, in many cases, catalytic activities for ORR about 1.5−3 times higher than that of pure Pt were reported. Moreover, the presence of a second element more abundant could contribute to decreasing of costs associated to Pt.

In a general manner, supported bimetallic catalysts Pt−M/C for cathodes have mainly been prepared by the deposition of the M precursor on Pt/C, followed by alloying at high temperature (usually above 700 °C). This thermal treatment produces, however, sintering of the particles with the concurrent increase of average particle size. More recently, some other procedures have been used attempting to minimize the undesired metal particle growth typically observed in the alloying method. Most commonly, simultaneous deposition and reduction of Pt and the second metal have been carried out using a variety of reducing agents, such as hydrazine,[6] formate,[5] formic acid,[24] and borohydride.[15,22,23,32] Other procedures such as precipitation of second metal as hydroxide,[9] incorporation of the second metal on Pt/C by sol−gel,[26] and synthesis via carbonyl complexes,[12,14,29,31] in microemulsions,[10] by the thermolysis of a single molecular precursor,[13] from a colloidal precursor (Bonnemann's method),[30] and by polyol methods in ethylene glycol solution have also been carried out.[7] While several supported Pt-based binary or ternary catalysts have been prepared by different methods, the ability to control the size and composition is limited because of the tendency of nanometric metal particles to aggregate. Moreover, in all cases mentioned above, the preparation of carbon-supported catalysts still involved a thermal treatment to promote reduction of the precursors or alloying, which as said before, produces particle growth. As result, literature data for Pt-based supported catalysts clearly show that the physical properties of the catalysts, such as particle size and distribution and degree of alloying, depend strongly on the preparation methodology.[35] These properties may, in turn, influence significantly the electrochemical performance.

In the so-called polyol process, developed by Fievet et al.,[36] a diol or polyalcohol (ethylene glycol or diethylene glycol) is used as both solvent and reducing agent of metallic precursors. This methodology has been used to prepare metallic[37] and bimetallic nanoparticles,[38−42] mainly for magnetic materials. The preparation of polycrystalline networks of nanoparticles of the ordered intermetallic phase of PtBi by a polyol method has also been reported.[43] This kind of synthetic route has also been used, with modifications such as addition of small amounts of water or NaOH, to prepare unsupported nanoclusters of Pt, Rh, and Ru,[44] Co−Cu nanocrystals,[45] carbon-supported Pt nanoparticles,[46] and carbon-supported Pt-based bimetallic catalysts.[7,47]

An interesting variation of this methodology was introduced by Sun et al.[48] that replaced the short-chain diol (ethylene glycol)

* To whom correspondence should be addressed. E-mail: mercedes@iq.unesp.br.

† Present address: PROCEL/IPEN-CNEN/SP, Av. Prof. Lineu Prestes, 2242 - Cidade Universitária, São Paulo (SP), Brazil. E-mail: eisantia@ipen.br.

10.1021/jp0670081 CCC: $37.00 
Published on Web 02/01/2007

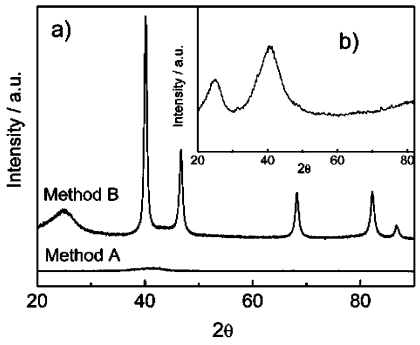


**Figure 1.** (a) X-ray diffraction patterns of $Pt_{70}Co_{30}$/C catalysts prepared by different methods (see text). (b) Enhanced X-ray diffraction pattern of $Pt_{70}Co_{30}$/C catalyst obtained by method A.

by a long-chain diol (hexadecanediol) to synthesize FePt nanoparticles by reduction of platinum acetylacetonate and decomposition of iron pentacarbonyl that are initiated together in the presence of oleic acid and oleyl amine stabilizers. The use of stabilizers provides a better control of the nucleation and growth process and, therefore, allows obtaining highly monodispersed nanoparticles. This kind of long-chain polyol method has also been used to prepare monodispersed FePt nanoparticles,[48,49] self-assembled FePt nanocrystals,[50] and monolayers of capped PtVFe nanoparticles.[51] However, to the best of our knowledge, studies of the electrochemical activity in PEMFC of carbon supported Pt-based materials prepared by the long-chain polyol process have not been previously reported.

In this work, $Pt_{70}Co_{30}$/C nanocatalysts were prepared by a polyol process on the basis of that proposed by Sun et al.,[48] and their electrochemical performance for oxygen reduction in single-cell PEMFC was evaluated. Depending on the synthesis conditions, highly monodispersed nanoparticles with very small size, high degree of alloying, and homogeneous distribution on the carbon support can be obtained without the need of any further thermal treatment.

## Experimental

**Electrocatalyst Synthesis.** $Pt_{70}Co_{30}$ nanoparticles were first obtained using a preparation methodology on the basis of the polyol method as proposed by Sun et al.[48] Thus, simultaneous reduction, in inert atmosphere, of platinum(II) acetylacetonate ($Pt(acac)_2$, Aldrich) and cobalt(II) acetylacetonate ($Co(acac)_2$, Aldrich) was carried out in the presence of 1,2 hexadecanediol, oleic acid, and oleylamine. Dioctyl ether was used as solvent. The synthesis was carried out using a modification of the usual approach.[50] Briefly, the synthesis was done as follows: $Pt(acac)_2$ and 1,2-hexadecanediol were mixed in dioctyl ether and were heated to 100 °C under nitrogen atmosphere. Subsequently, oleic acid, oleylamine, and an adequate amount of a solution of $Co(acac)_2$ in isopropanol preheated at 70 °C were added. The resulting mixture was then heated until reflux (298 °C) and was kept at that temperature for 30 min, when the formation of a black dispersion was observed. The heat source was removed and the dispersion was allowed to cool to room temperature. Ethanol was used as flocculent agent. The nanoparticles were separated by centrifugation and were redispersed in hexane, were precipitated with ethanol, and were separated by centrifugation several times, until a limpid solution was obtained. After this cleaning procedure, an excess of oleic acid and oleylamine was added before the carbon-supporting step. We shall refer to this preparation procedure as method A. For the sake of comparison, $Pt_{70}Co_{30}$ nanoparticles were also prepared by the usual method that involves the simultaneous addition of the metal precursor ($Pt(acac)_2$ and $Co(acac)_2$) to a solution of 1,2 hexadecanediol, oleic acid, and oleylamine in octyl ether at room temperature, followed by the same heating procedure (100 °C/10 min and reflux at 298/30 min) described above. We shall refer to this procedure as method B.

The $Pt_{70}Co_{30}$ nanoparticles were anchored on carbon powders (Vulcan XC-72, Cabot) previously treated at 850 °C/5 h in argon atmosphere[52] by constant stirring in hexane media for 2 h. The resulting material was filtered and dried at 85 °C for 2 h. All the materials were 20 wt % metal on carbon. In some cases, the supported catalysts were also submitted to heat treatment.

**Physical Characterization Techniques.** X-ray diffractograms of the electrocatalysts were obtained in a universal diffractometer Carl Zeiss-Jena, URD-6, operating with Cu K$\alpha$ radiation ($\lambda = 1.5406$ Å) generated at 40 kV and 20 mA. Scans were done at 2 $min^{-1}$ for $2\theta$ values between 20° and 100°.

The transmission electronic microscopy (TEM) study was done using a Philips CM 200 microscope operating at 200 kV, coupled to an energy dispersive X-ray analysis (EDX) spectrometer. The samples for the TEM analysis were prepared by ultrasonically dispersing the catalyst powders in ethanol. A drop of the suspension was applied onto a carbon-coated copper grid and was dried in air.

**Fuel Cell Measurements.** Catalyst layers of gas diffusion electrodes for single PEMFC were prepared as described elsewhere.[53] The total metal loading was 0.4 mg $cm^{-2}$ for both anode (Pt/C, 20 wt % E-TEK) and cathode (PtCo/C). In all cases, 35.5 wt % of Nafion (5 wt % solution in a mixture of alcohols, DuPont) was applied to the catalyst layer. The gas diffusion layer consisted of carbon powder (Vulcan XC-72R, Cabot) with 15 (w/w) polytetrafluoroethylene (PTFE, TE-306A, DuPont) deposited onto a carbon cloth substrate (PWB-3, Stackpole). Membrane and electrode assemblies (MEAs) were prepared by hot pressing the anode and the cathode to a membrane of Nafion ($H^+$, N115, DuPont) at 125 °C and 1000 kgf $cm^{-2}$ for 2 min.

Fuel cell polarization measurements were carried out galvanostatically with the single cell at 80 °C, using oxygen saturated with ultrapure water (18MΩ, Milli-Q) at 85 °C and pure hydrogen saturated with water at 95 °C. All measurements were obtained at 1 atm of overall pressure. Before the data acquisition, the system was kept at 0.7 V for 2 h to reach the steady-state condition.

Cyclic voltammograms were performed on the gas diffusion electrodes using a potentiostat-galvanostat (1285, Solartron). In these experiments, the cathode was used as working electrode while the anode, to which a continuous injection of pure hydrogen was applied, was used as counter and reference (RHE) electrodes.

## Results and Discussion

The composition of the $Pt_{70}Co_{30}$/C electrocatalysts was determined by EDX analysis. The actual composition ($Pt_{73}Co_{27}$)

**TABLE 1: Structural Characteristics of the $Pt_{70}Co_{30}$/C Catalysts**

| $Pt_{70}Co_{30}$/C | crystallite size by XRD (nm) | lattice parameter (nm) | degree of alloying (%) | Pt−Pt distance (nm) |
|---|---|---|---|---|
| method A | 1.8 | 0.3501 | 79 | 0.248 |
| method B | 24.4 | 0.3889 | 40 | 0.275 |

was found to be very close to the nominal value, indicating a good incorporation of Co into the catalyst.

The results of X-ray diffraction (XRD) for $Pt_{70}Co_{30}$/C electrocatalysts are shown in Figure 1. The broad peak at $2\theta$ approximately 25° is characteristic of the carbon support. The XRD patterns for all electrocatalysts prepared by method B are very similar to that for Pt/C, without any additional peaks, indicating that the PtCo/C catalysts have the face-centered cubic (fcc) structure of platinum (JCPDS 04-802). The diffraction peaks are shifted toward higher $2\theta$ values compared to those of Pt, indicating Pt−Co alloy formation. For all samples prepared in this work, diffraction signals that could be associated to the presence of crystalline cobalt or cobalt oxides were not observed. In contrast with the XRD data of the catalyst prepared by method B, the diffraction pattern for the as-prepared $Pt_{70}Co_{30}$/C electrocatalyst obtained by method A appears to be featureless. However, closer inspection (Figure 1b) of these XRD data reveals the presence of a wide diffraction peak centered at $2\theta$ around 40° that corresponds to the diffraction of [111] planes, while signals at $2\theta$ values of about 46° and 67° are absent.

Very recently, Borchert et al.[54] demonstrated that for highly monodispersed nanoparticles, particle sizes estimated from the line broadening of XRD reflections according to Scherrer's equation agreed within 5% with the values obtained from TEM and SAXS (small-angle X-ray scattering) measurements, when Scherrer's equation was adapted to spherical geometry as

$$d = \frac{4}{3}\frac{0.9\lambda}{\omega \cos\theta} \quad (1)$$

where $d$ is the average particle diameter, $\lambda$ is the wavelength of the X-ray radiation (1.54056 Å), $\omega$ is the width of the diffraction peak at half intensity (in radians), and $\theta$ is the angle of the considered Bragg reflection. The estimated mean crystallite sizes using eq 1 and the diffraction peak at ~40° were 1.8 and 24.4 nm, for catalysts prepared by method A and method B, respectively.

The very small mean crystallite size obtained for the PtCo/C catalysts prepared by method A (1.8 nm) could explain the broad diffraction signal around $2\theta \sim 40°$ as well as the absence of other diffraction peaks expected for Pt. Early works on small particle effects[55] show that the relationship between the number of surface atoms ($N_S$) and the number of total atoms ($N_T$) in the metal particle becomes equal to 1 when particle diameter is ≤1 nm, that is, every atom in the metal particle becomes a surface atom. Considering particles with a cuboctahedral structure, Kinoshita[56] has shown that the mass-averaged distribution (MAD), the distribution of surface atoms normalized to the total number of atoms in the particle, shows a maximum for the (111) crystal face for particle size of ~2 nm and that the distribution of atoms on the (111) face is about 10 times higher than that on the (100) face. Additionally, it has been suggested that very small particles could have thermodynamically stable structures different from those expected for the macroscopic material and that very small particles of fcc metals could have icosahedral structures consisting primarily of [111] triangular surfaces.[55]

The degree of alloying of the $Pt_{70}Co_{30}$/C electrocatalysts was estimated assuming that the variation of lattice parameter on Co content follows Vegard's law:

$$x_{(Co)} = \frac{(a_o - a_{exp})}{a_{alloy} - a_o} \quad (2)$$

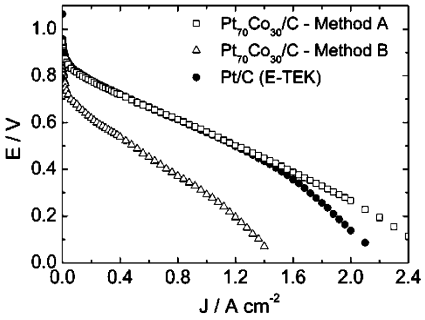


**Figure 2.** $H_2/O_2$ PEM fuel cell polarization curves with $Pt_{70}Co_{30}$/C electrocatalysts and commercial Pt/C for oxygen reduction at 80 °C and 1 atm. Catalyst layer with metal loading 0.4 mg $cm^{-2}$. Anodes were made with commercial Pt/C electrocatalyst.

where $a_{exp}$ is the experimental value of lattice parameter for the PtCo/C catalysts, and $a_o$ and $a_{alloy}$ are the lattice parameters of supported Pt and $Pt_3Co$ alloy, taken here as 3.927 Å and 3.831 Å, respectively.[57] The values of the lattice parameter and of the Pt−Pt distances for the Pt−Co materials were smaller than for Pt, in agreement with the expected contraction of the lattice because of the partial substitution of Pt by Co in the fcc structure. Results are summarized in Table 1.

The marked differences in the XRD patterns and in average crystallite size reveal the importance of synthesis conditions. While method B is the usually adopted route in polyol synthesis, that is, the solid metal precursors are both added to the octyl ether solvent at the beginning of the procedure, method A involves the addition of a solution of the Co precursor after the reaction medium has reached a given temperature (~100 °C). Even though at first sight this difference could be considered a minor variation of the synthesis conditions, the results show that method A allows a better control of the nucleation and growth processes, leading to significantly smaller particles. This observation could be related to the rather limited solubility of $Co(acac)_2$ in octyl ether at low temperatures. Gradual dissolution of the metal precursor could introduce inhomogeneities because of the presence of undissolved solid or of a varying cobalt concentration in the reaction medium.

Figure 2 shows the polarization curves for a single PEMFC using the as-prepared $Pt_{70}Co_{30}$/C electrocatalysts as cathodes. A curve taken using a commercial Pt/C catalyst (20% Pt, E-TEK) as cathode material is included for comparison. The pronounced difference in performance between the catalysts prepared by method A and method B can be ascribed to the significant differences in average crystallite size and degree of alloying.

The most important aspect of the results presented in Figure 2 is that, despite its lower Pt content, the performance of the as-prepared $Pt_{70}Co_{30}$/C catalyst obtained by method A is very close to that of the commercial Pt/C catalyst. All cathodes were prepared with identical metal load (0.4 mg/$cm^2$), that is, the amount of Pt in the $Pt_{70}Co_{30}$/C cathodes is 70% of the amount of Pt used in the Pt/C electrode. Since the cost of cathode depends on the amount of Pt used, the catalyst's mass activity (MA), that is, the current density per mg of Pt, is an important parameter because of its practical implications. As it can be seen in Figure 3, the $Pt_{70}Co_{30}$ has a superior performance in terms of MA.

Figures 4 and 5 show TEM images of the carbon-supported $Pt_{70}Co_{30}$ nanoparticles prepared by method A and the corresponding particle size distribution histogram. As it can be seen, the metal nanoparticles are homogeneously dispersed on the surface of the carbon support, which could be associated to the

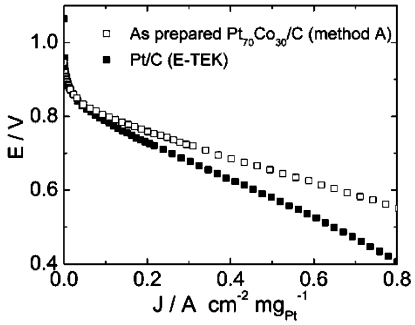


**Figure 3.** $H_2/O_2$ PEM fuel cell polarization curves with $Pt_{70}Co_{30}/C$ electrocatalysts and commercial Pt/C for oxygen reduction at 80 °C and 1 atm. Currents are expressed in terms of mass activity (MA). Anodes were made with commercial Pt/C electrocatalyst.

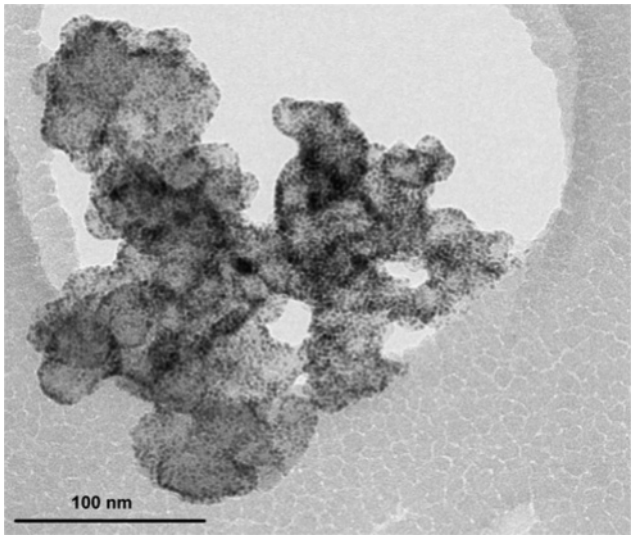


**Figure 4.** TEM micrographs of the $Pt_{70}Co_{30}/C$ prepared by method A.

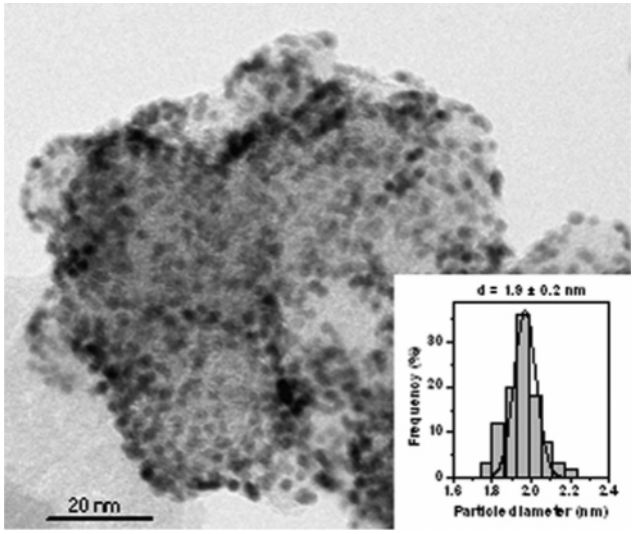


**Figure 5.** TEM micrographs of the $Pt_{70}Co_{30}/C$ prepared by method A and histogram of metal particle size distribution.

presence of an excess of stabilizers, and exhibit a very narrow particle size distribution. The mean particle size is 1.9 ± 0.2 nm, in excellent agreement with the average crystallite size calculated from XRD data and eq 1. *To the best of our knowledge, compared with literature values, this is the smallest average particle diameter reported for Pt−Co catalysts.*

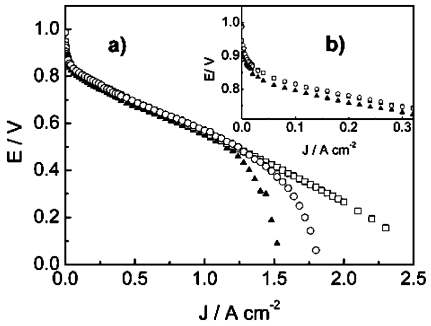


**Figure 6.** (a) $H_2/O_2$ PEM fuel cell polarization curves with $Pt_{70}Co_{30}/C$ electrocatalysts for oxygen reduction at 80 °C and 1 atm. (●) as-prepared $Pt_{70}Co_{30}/C$ catalyst obtained by method A, (○) heat-treated (air/$H_2$), (▲) commercial PtCo (3:1)/C (E-TEK). Catalyst layer with metal loading 0.4 mg $cm^{-2}$. Anodes were made with commercial Pt/C electrocatalyst. (b) Initial portion of polarization curves.

According to Kinoshita,[56] the dependence of the mass activity for oxygen reduction on Pt particle size shows a maximum at $d = 3.5$ nm, coincident with the maximum of the mass-averaged distribution (MAD) for the (100) planes. The performance of the $Pt_{70}C_{30}/C$ catalyst prepared by method A shown in Figures 2 and 3 is surprisingly good when analyzed in terms of the average particle size (1.9 ± 0.2 nm). This makes evident that particle size is not the only factor that determines the electrocatalytic activity for ORR. Therefore, in an attempt to analyze alloying effects, the result of thermally treating $Pt_{70}C_{30}/C$ catalysts obtained by method A was also evaluated. In a general manner, thermal treatment, even at relatively low temperatures (200−400 °C), produced particle growth, as expected. For instance, heat treatment in hydrogen atmosphere at 400 °C (2 h) led to an increase in the average crystallite size up to 9.6 nm, an increase in the lattice parameter to 0.390 nm, and a significant loss of performance in PEMFC measurements. The effects of combining heat treatments in oxidizing and reducing atmospheres were also investigated. Thus, the $Pt_{70}C_{30}/C$ catalysts prepared by method A were first heated in air at 200 °C (1 h) and were subsequently heated in hydrogen at 300 °C (1 h). As result, the average crystallite size increased up to 8.3 nm, the lattice parameter increased to 0.390 nm, indicating a lower degree of alloying probably associated to cobalt oxidation, while the performance as PEMFC cathode remained basically identical until a potential of ∼0.5 V, as shown in Figure 6. The only significant difference is related to the appearance of diffusion limitations that set in at lower current densities for the heat-treated sample, which could be related to electrode characteristics and not to intrinsic properties of the catalyst. A curve obtained using PtCo 3:1 commercial catalyst cathode is included for comparison. It seems quite clear that the performance of both as-prepared and thermally treated (air/$H_2$) $Pt_{70}Co_{30}/C$ catalysts prepared by method A is slightly superior to that of the Pt−Co (3:1)/C commercial catalyst.

Figure 7 shows the cyclic voltammograms taken at 50 mV $s^{-1}$ for the as-prepared and heat-treated (air/$H_2$) $Pt_{70}Co_{30}/C$ electrocatalysts. As it can be seen, curve of the heat-treated catalyst involves a significantly lower charge in the Pt adsorption/desorption region, consistent with the larger value of particle size. Faradaic currents in the double region are quite apparent. This oxidation/reduction process serves as indication of the presence of significant amounts of cobalt oxide. Despite the obvious differences in the cyclic voltammograms that clearly evidence marked differences in the electroactive areas and in the amounts of cobalt oxides at the electrode surface,

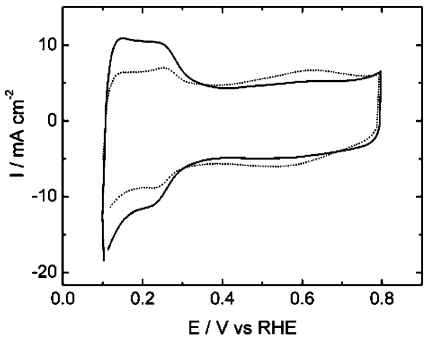


**Figure 7.** Cyclic voltammograms for as-prepared (—) and heat-treated (·····) $Pt_{70}Co_{30}$/C catalyst obtained by method A.

the performance of both materials is surprisingly similar (Figure 6).

Even though there is agreement about the influence of particle shape, size, and size distribution on the kinetics of the ORR, many questions regarding these aspects remain to be answered. Jalan and Taylor[58] proposed that the Pt−Pt nearest-neighbor distance was the main factor affecting the catalytic activity for oxygen reduction reaction from studies of various platinum alloys. Min et al.[18] concluded that particle size and alloying are the two most important factors affecting the catalytic activity toward oxygen reduction reaction. The effect of alloying on OH adsorption on the Pt−M surface (M = Ni, Co, Fe, and Cr) has also been examined and the OH inhibition was correlated with kinetic reactivity for a fuel cell with those bimetallic materials.[59] Some authors have suggested that the enhanced activity for ORR on bimetallic surfaces may arise from the formation of a Pt skin.[60−62] From extended X-ray absorption fine structure (EXAFS) studies, Teliska et al.[59] concluded that, while the Pt−Fe and Pt−Cr samples have a Pt skin, their Pt−Ni and Pt−Co clusters were more homogeneous with M atoms on the surface. The formation of a Pt skin was observed for all samples after annealing at high temperature. Studying Pt−Co catalysts and the ORR, Antolini et al.[25] concluded that the activity of their catalysts could not be explained in terms of either Co content, Pt−Pt distance, or as a function of particle size, pointing out the mutual influence among these parameters. They found, however, that the observed activities were related to OH adsorption that was, in turn, reduced by the increase of particle size and Co content in the alloy.

The performances of the as-prepared and heat-treated $Pt_{70}Co_{30}$/C catalysts obtained by method A (Figure 6) are almost identical despite the fact that the as-prepared electrocatalyst has a very small particle size (1.9 nm) together with a considerably high degree of alloying, while the heat-treated $Pt_{70}Co_{30}$/C catalyst has a significantly larger particle size (8.3 nm) and a lower degree of alloying ($a = 0.3897$ nm) with the concomitant increase in the Pt−Pt distance, as well as some cobalt in the form of oxide, as evidenced by the cyclic voltammetry (CV) curves of Figure 7. Considering that for 2-nm nanoparticles about 50% of the atoms would be at the surface,[55,56] the formation of a Pt skin on the as-prepared $Pt_{70}Co_{30}$/C catalysts obtained by method A seems unlikely because of the high degree of alloying observed. These results cannot be rationalized in terms of a single dominant effect (particle size, alloying, surface oxides, etc). However, a combination of these effects might contribute to a superior and stable performance during continuous polarization.

Much effort in this area is still needed to understand the way in which all parameters combined affect the catalytic properties of PtM/C cathode materials.

## Conclusions

$Pt_{70}Co_{30}$/C catalyst with very small particle size (1.9 ± 0.2 nm) and narrow distribution was obtained by a polyol method with a long-chain diol as reducing agent. To the best of our knowledge, compared with literature values, this is the smallest average particle diameter reported for Pt−Co catalysts. The $Pt_{70}Co_{30}$ nanoparticles were found to be homogeneously dispersed on the carbon support and have a high degree of alloying. The as-prepared catalyst presents an excellent performance as PEMFC cathode material without the need of any further heat treatment.

**Acknowledgment.** The authors thank the financial support of the Fundação de Amparo a Pesquisa do Estado de São Paulo (FAPESP, Procs. 04/15570-8, 04/04555-8, 04/02407-1), the Conselho Nacional de Desenvolvimento Científico e Tecnológico (CNPq, Proc. 550153/2005-5), and the Procac Program. Thanks are due to Prof. Ernesto R. Gonzalez and Prof. Edson A. Ticianelli (IQSC-USP, Brazil) for the use of their laboratory for PEMFC measurements. L.C.V. thanks FAPESP for a research fellowship.

## References and Notes

(1) Gasteiger, H. A.; Gu, W.; Makharia, R.; Mathias M. F.; Sompalli, B. In *Handbook of Fuel Cells: Fundamentals, Technology, and Applications*; Vielstich, W., Lamm, A., Gasteiger, H. A., Eds.; Vol. 3; Wiley: New York, 2003; Chapter 46, p 593.

(2) Mukerjee, S.; Srinivasan, S.; Soriaga, M. P.; McBreen, J. *J. Electrochem. Soc.* **1995**, *142*, 1409.

(3) Toda, T.; Igarashi, H.; Watanabe, M. *J. Electroanal. Chem.* **1999**, *460*, 258.

(4) Toda, T.; Igarashi, H.; Uchida, H.; Watanabe, M. *J. Electrochem. Soc.* **1999**, *146*, 3750.

(5) Xiong, L.; Kannan, A. M.; Manthiram, A. *Electrochem. Commun.* **2002**, *4*, 898.

(6) Shukla, A. K.; Raman, R. K.; Choudhury, N. A.; Priolkar, K. R.; Sarode, P. R.; Emura, S.; Kumashiro, R. *J. Electroanal. Chem.* **2004**, *563*, 181.

(7) Li, W.; Zhou, W.; Li, H.; Zhou, Z.; Zhou, B.; Sun, G.; Xin, Q. *Electrochim. Acta* **2004**, *49*, 1045.

(8) Murthi, V. S.; Urian, R. C.; Mukerjee, S. *J. Phys. Chem. B* **2004**, *108*, 11011.

(9) Xiong, L.; Manthiram, A. *J. Electrochem. Soc.***2005**, *152*, A697.

(10) Xiong, L.; Manthiram, A. *Electrochim. Acta* **2005**, *50*, 2323.

(11) Stamenkovic, V.; Schmidt, T. J.; Ross, P. N.; Markovic, N. M. *J. Electroanal. Chem.* **2003**, *554*, 191.

(12) Yang, H.; Vogel, W.; Lamy, C.; Alonso-Vante, N. *J. Phys. Chem. B* **2004**, *108*, 11024.

(13) Deivaraj, T. C.; Lee, J. Y. *J. Electrochem. Soc.* **2004**, *151*, A1832.

(14) Yang, H.; Coutanceau, C.; Leger, J.-M.; Alonso-Vante, N.; Lamy, C. *J. Electroanal. Chem.* **2005**, *576*, 305.

(15) Antolini, E.; Salgado, J. R. C.; dos Santos, A. M.; Gonzalez, E. R. *Electrochem. Solid-State Lett.* **2005**, *8*, A226.

(16) Paulus, U. A.; Wokaun, A.; Scherer, G. G.; Schmidt, T. J.; Stamenkovic, V.; Radmilovic, V.; Markovic, N. M.; Ross, P. N. *J. Phys. Chem. B* **2002**, *106*, 4181.

(17) Stamenkovic, V.; Schmidt, T. J.; Ross, P. N.; Markovic, N. M. *J. Phys. Chem. B* **2002**, *106*, 11970.

(18) Min, M.; Cho, J.; Cho, K.; Kim, H. *Electrochim. Acta* **2000**, *45*, 4211.

(19) Obradovic, M. D.; Grgur, B. N.; Vracar, Lj. M. *J. Electroanal. Chem.* **2003**, *548*, 69.

(20) Koponen, U.; Kumpulainen, H.; Bergelin, M.; Keskinen, J.; Peltonen, T.; Valkiainen, M.; Wasberg, M. *J. Power Sources* **2003**, *118*, 325.

(21) Salgado, J. R. C.; Antolini, E.; Gonzalez, E. R. *J. Electrochem. Soc.* **2004**, *151*, A2143.

(22) Salgado, J. R. C.; Antolini, E.; Gonzalez, E. R. *J. Power Sources* **2004**, *138*, 56.

(23) Salgado, J. R. C.; Antolini, E.; Gonzalez, E. R. *J. Phys. Chem. B* **2004**, *108*, 17767.

(24) Salgado, J. R. C.; Antolini, E.; Gonzalez, E. R. *J. Power Sources* **2005**, *141*, 13.

(25) Antolini, E.; Salgado, J. R. C.; Giz, M. J.; Gonzalez, E. R. *Int. J. Hydrogen Energy* **2005**, *30*, 1213.

(26) Soderberg, J. N.; Sirk, A. H. C.; Campbell, S. A.; Birss, V. I. *J. Electrochem. Soc.* **2005**, *152*, A2017.
(27) Takasu, Y.; Matsuyama, R.; Konishi, S.; Sugimoto, W.; Murakami, Y. *Electrochem. Solid-State Lett.* **2005**, *8*, B34.
(28) Neergat, M.; Shukla, A. K.; Gandhi, K. S. *J. Appl. Electrochem.* **2001**, *31*, 3373.
(29) Yang, H.; Alonso-Vante, N.; Leger, J.-M.; Lamy, C. *J. Phys. Chem. B* **2004**, *108*, 1938.
(30) Leger, J.-M. *Electrochim. Acta* **2005**, *50*, 3123.
(31) Yang, H.; Alonso-Vante, N.; Lamy, C.; Akins, D. L. *J. Electrochem. Soc.* **2005**, *152*, A704.
(32) Antolini, E.; Salgado, J. R. C.; Santos, L. G. R. A.; Garcia, G.; Ticianelli, E. A.; Pastor, E.; Gonzalez, E. R. *J. Appl. Electrochem.* **2006**, *36*, 355.
(33) Cambanis, G.; Chadwick, D. *Appl. Catal.* **1986**, *25*, 191.
(34) Antolini, E.; Passos, R. R.; Ticianelli, E. A. *Electrochim. Acta* **2002**, *48*, 263.
(35) Antolini, E. *Mater. Chem. Phys.* **2003**, *78*, 563.
(36) Fievet, F.; Lagier, J. P.; Figlarz, M. *MRS Bull.* **1989**, *14*, 29.
(37) Yan, X. P.; Liu, H. F.; Liew, K. Y. *J. Mater. Chem.* **2001**, *11*, 3387.
(38) Toshima, N.; Wang, Y. *Langmuir* **1994**, *10*, 4574.
(39) Chow, G. M.; Kurihara, L. K; Kemmer, K. M.; Schoen, P. E.; Elam, W. T.; Ervin, A.; Keller, S.; Zhang, Y. D.; Budnick, J.; Ambrose, T. *J. Mater. Res.* **1995**, *10*, 6.
(40) Viau, G.; Fievet-Vincent, F.; Fievet, F. *Solid State Ionics* **1996**, *8*, 259.
(41) Lu, P.; Dong, J.; Toshima, N. *Langmuir* **1999**, *15*, 7980.
(42) Bonet, F.; Grugeon, S.; Dupont, L.; Herrera, Urbina, R.; Guery, C.; Tarascon, J. M. *J. Solid State Chem.* **2003**, *172*, 111.
(43) Roychowdhury, C.; Matsumoto, F.; Mutolo, P. F.; Abruña, H. D.; DiSalvo, F. *J. Chem. Mater.* **2005**, *17*, 5871.
(44) Wang, Y.; Ren, J.; Deng, K.; Gui, L.; Tang. Y. *Chem. Mater.* **2000**, *12*, 1622.
(45) Sra, A. K.; Ewers, T. D.; Schaak, R. E. *Chem. Mater.* **2005**, *17*, 758.
(46) Zhou, Z. H.; Wang, S. L.; Zhou, W. J.; Wang, G. X.; Jiang, L. H.; Li, W. Z.; Song, S. Q.; Liu, J. G.; Sun, G. Q.; Xin, Q. *Chem. Commun.* **2003**, *3*, 394.
(47) Zhou, W.; Zhou, Z.; Song, S.; Li, W.; Sun, G.; Tsiakaras, P.; Xin, Q. *Appl. Catal. B* **2003**, *46*, 273.
(48) Sun, S.; Murray, C. B.; Weller, D.; Folks, L.; Moser, A. *Science* **2000**, *287*, 1989.
(49) Liu, C.; Wu, X. W.; Klemmer, T.; Shukla, N.; Yang, X. M.; Weller, D.; Roy, A. G.; Tanase, M.; Laughlin, D. *J. Phys. Chem. B* **2004**, *108*, 6121.
(50) Varanda, L. C.; Jafelicci, M. *J. Am. Chem. Soc.* **2006**, *128*, 11062.
(51) Luo, J.; Han, L.; Kariuki, N. N.; Wang, L.; Mott, D.; Zhong, C.-J.; He, T. *Chem. Mater.* **2005**, *17*, 5282.
(52) Pinheiro, A. L. N.; Oliveira-Neto, A.; de-Souza, E. C.; Perez, J.; Paganin, V. A.; Ticianelli, E. A.; Gonzalez, E. R. *J. New Mater. Electrochem. Syst.* **2003**, *6*, 1.
(53) Paganin, V. A.; Ticianelli, E. A.; González, E. R. *J. Appl. Electrochem.* **1996**, *26*, 297.
(54) Borchert, H.; Shevchenko, E. V.; Robert, A.; Mekis, I.; Kornowski, A.; Grubel, G.; Weller, H. *Langmuir* **2005**, *21*, 1931.
(55) Kinoshita, K. In *Modern Aspects of Electrochemistry*; Bockris, J. O'M., Conway, B. E., White, R. E., Eds.; Wiley: New York, 1982; No. 14, p 557.
(56) Kinoshita, K. *J. Electrochem. Soc.* **1990**, *137*, 845.
(57) Beard, B. C.; Ross, P. N. *J. Electrochem. Soc.* **1990**, *137*, 3368.
(58) Jalan, V.; Taylor, E. J. *J. Electrochem. Soc.* **1983**, *130*, 2299.
(59) Teliska, M.; Murthi, V. S.; Mukerjee, S.; Ramaker, D. E. *J. Electrochem. Soc.* **2005**, *152*, A2159.
(60) Toda, T.; Igarashi, H.; Watanabe, M. *J. Electroanal. Chem.* **1999**, *460*, 258.
(61) Toda, T.; Igarashi, H.; Uchida, H.; Watanabe, M. *J. Electrochem. Soc.* **1999**, *146*, 3750.
(62) Stamenkovic, V.; Schmidt, T. J.; Ross, P. N.; Markovic, N. M. *J. Electroanal. Chem.* **2003**, *554*−*555*, 191.